PLEA 2017 EDINBURGH
Design to Thrive

Experimental study of the roof thermal performance influence over the mean radiant interior temperature of an industrial building

Jefferson Torres[1], Helena Coch[1], Isabel Crespo[1] and Antonio Isalgué[2]

[1] Architecture & Energy, School of Architecture, Polytechnic University of Catalonia, Barcelona, Spain, Av. Diagonal, 649, 7th floor. 08028;
[2] Applied Physics Department, Polytechnic University of Catalonia, Barcelona, Spain, Pla del Palau, 18. 08003.

Abstract: Industrial building rehabilitation is one the latest trends within the field of sustainable development. However, these interventions often disregard the issue of user comfort, despite being the most important factor of energy efficiency. This work deals with the assessment of the indoor thermal conditions of a restored industrial building, considering not only air temperature but also mean radiant interior temperature. The research focuses in the influence of the radiative performance of the saw tooth roof of this building regarding these conditions. Results show that the analysed thermal parameters depend directly on the roof thermal behaviour. In fact, the glazed area of this type of roof is responsible for the 60% of the increase of the mean radiant temperature over air temperature. This result is a consequence of the high interior temperature reached by the glass panels, 47°C max, despite their northern orientation. These temperatures are a result of the diffuse radiation action and, particularly, the heat flux emitted by the opaque part of the saw tooth-roof, which significantly reduces the radiative cooling capacity of the glazed surface.

Keywords: Industrial building, mNACTEC, Mean radiant temperature, Saw-tooth roof.

Introduction

The industrial revolution, being one of the most significant changes in the history of humankind (Andrei, 2012), brought as a consequence the development of a new building typology. Large manufacturing spaces with proper lighting-spatial conditions for the implementation of productive activities were needed.

Some of these buildings have left their mark on contemporary cities through some examples of technological and aesthetic value (Fernández et al, 2016). Furthermore industrial heritage has impacted not only tangible aspects, but intangible factors too like the collective memory and identity of a place (Sutestad et al, 2016). These buildings accumulate materials, energy, and the human effort that made them possible. Their conservation and recycling for new uses is nowadays a challenge (Romeo et al, 2015).

Vapor Aymerich, Amat i Jover, designed by architect L. Muncunill, was built in 1908 in Terrassa (Spain) to operate as a textile industry, being a case of industrial architecture. This building has been restored in 1992 and converted to the Catalonia Science and Technology Museum (mNACTEC). It had a production area around 11,000 m2 which has become the principal exhibition hall of the Museum after its rehabilitation. Due to its initial purpose, the elaboration of fine textiles, this space was provided with a roof in saw-tooth. This type of roof, with its glass panels facing north, provides a large amount of natural light, and avoids

the access of direct solar radiation to the interior. However, after the rehabilitation and used as Museum, the thermal indoor conditions are considered too hot in summer by visitors and workers, in spite of the scarce of sunlight entering.

The preservation of industrial buildings is considered a sustainable approach. However, the mNACTEC rehabilitation disregards its new museum's use and this could became a contradiction in terms of energy efficiency. Industrial buildings should be rehabilitated in order to be adapted to their new uses with the purpose to improve their conditions adapted to the current standards and requirements (Blagojević et al, 2016).

Even energy saving is one of the main aim in building sector, the user indoor conditions should be considered in any construction (Kalmár et al, 2011). The most important variables in regards of thermal comfort conditions are: air temperature, relative humidity, wind velocity and the mean radiant temperature (Givoni, 1994) (Walikewitz et al, 2015). Several researches have studied the influence of hot air temperatures in the interior comfort conditions on residential buildings (Beizaee et al, 2013)(Mirzaei et al, 2012). Other studies approach this issue focusing in the mean radiant temperature, assessing issues like its influence on the indoor thermal environment (d'Ambrosio et al, 2013), the interrelation with the room geometry (Kalmár et al, 2012) or the comfort limits for heated ceilings (Fanger et al, 1980). Likewise, Atmaca argues that the mean radiant temperature is a very significant factor especially in buildings whose envelopes are exposed to a strong solar radiation (Atmaca et al, 2007), like is the case of the mNACTEC roof.

In this sense, due to the proportion that the roof represents with respect to the indoor space and the singularity of its own geometry, a detailed analysis of the radiative performance of this element will be recommended.

This work addresses the issue of the interior thermal conditions, considering the possible influence of the mean radiant temperature. The specific aim of this research is to assess the influence of the radiative performance of the building saw-tooth roof, evaluating the thermal repercussions of the opaque and glass envelope surfaces.

Methodology

The methodology is based on an experimental work carried out in the mNACTEC during a period in the hottest period of summer 2015. The building is located in Terrassa-Spain, at 2°00´E, 41°33´N and 286 masl, which lies in the Mediterranean climatic zone.

The building has a main exhibition hall, 11000 m2, with 161 Catalonians vaults arranged in a grid of 7 modules in the East-West direction and by 23 modules in the North-South direction covered by a saw-tooth roof. Every module of the roof is composed by two parts: an opaque and a glass surface. The opaque surface is a semi-vault defined by a double bent built in brick. It has a 0.33m thickness composed by various layers of bricks with an air gap in the middle as shown in Figure 1c. The glass surface, oriented almost to the North (19° to the West), is formed by two simple glass panels separate by an air gap.

The experimental work of analysis of the roof radiative performance influence on the mean radiant indoor temperature has been divided in two parts. The first part focuses on the roof thermal behaviour and the second part on the thermal interior conditions. The roof measurements had the purpose to assess its thermal response to the climatic conditions to which it is exposed. Due to the singularity of its geometry the two surfaces, opaque and glazed, had been analysed separately. Solar radiation (SR), long-wave radiation (LW) and surface temperatures Ts of the opaque and glass parts (Ts.op, Ts.g) were measured, outside and inside, on this two elements that comprise the roof. The second part addresses the

ambient interior conditions in order to match these results with the roof thermal behaviour. The parameters considered in this part were the mean radiant interior temperature (Tmrt) and indoor air temperature (Tai). It has been analysed the independent influence of the glass and opaque surface over the mean radiant temperature through calculations.

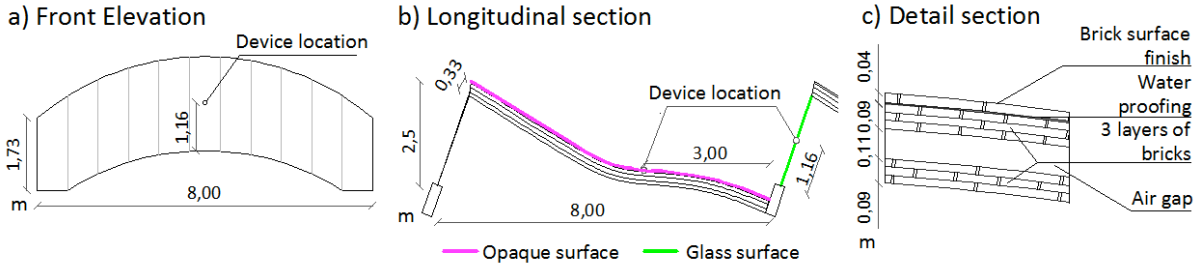

Figure 1. Construction specifications a) Front elevation b) longitudinal section and c) detail section.

The module selected from the grid to be measured was the tenth from North, and the third from West. The data of the glass surface, SR and LW was collected from June 23th to June 30th, and the outdoor surface temperature from July 1st to July 8th. The three same parameters were measured on the opaque surface from July 1st to July 8th. The data are always referred to solar time (UTC). The equipment used was: for SR a pyranometer MS-020VM with a spectral range from 350nm to 1100nm, for LW a pyrgeometer IR02 with a spectral range from 4.5 µm to 40 µm and a field view angle of 150° connected to a data logger CR800, and for the surface temperatures an external thermocouple K-type connect to a multifunctional meter TESTO 435. The first two instruments were set to collect data in 5 min and the last in 20 min intervals. Due to the difficulty of measuring the indoor temperature of the glass and opaque surfaces, an infrared thermometer was used, spectral range 8-14 µm, and emissivity calibrated at 0.90. In order to make a proper diagnostic of the radiative roof behaviour, due to the complexity of its geometry, measurements in 9 different points over glass an opaque surface were done. The measurements were done outside and inside on both surfaces, on July 9th from 09:00h to 18:00h every 30 min. This procedure was supported through thermal images with the use of a thermo-graphic-camera FLIR I7. These measurements of radiant temperatures were validated comparing the outside surface temperatures measured with the infrared thermometer and the K-type thermocouples, and the average differences were less than 0.7°C.

In regards to the ambient indoor measurements, all parameters considered in this part were collected from July 9th to July 13th. In order to assess Tmrt under indoor conditions, a frequent method validated in several studies was used (Thorsson et al, 2007) (d'Ambrosio et al, 2013) which involved the globe temperature, air temperature and air velocity. The globe and air temperature were measured using a globe thermometer WB 20SD; for the air velocity an anemometer HIBOK AM8901 range from 0.4-35 m/sec. All the equipment was placed at 2.10 m height, out of visitors' reach. The data was collected at 10 min and 60 min intervals respectively.

Finally, outdoor air temperature data was gathered from the database of the nearest Weather Station from the Museum ID: ITERRASS3, located at 300m from the building at 2°00´48´´E, 41°33´59´´N and 307 masl. The information was collected in 20 min intervals.

The data were collected in 3 different periods but with the aim to make a comparable analysis, 1 day from each period with similar climatic conditions has been chosen, June 29th, July 1st and July 9th. All these days had clear sky conditions, with mean temperatures and SR of 28.8ºC, 360 W/m2; 28.6ºC, 330 W/m2; and 27.5ºC and 332 W/m2.

Results and discussion: Roof.

Figure 2 shows the results of the radiation heat flux data on the opaque surface (a) and glazed surface (b). Regarding to the results for opaque surface, it shows a SR curve with no interruptions, which reflected 0% obstructions, and completely clear sky conditions throughout the whole day. This radiation appears at 04:30h, it rises until its peak 1000 W/m^2 at 12:00h, and then it starts to fall down until disappearing at 19:30h. In regards to the LW at night periods from 00:00 h to 04:30 h and 19:30 h to 24:00 h the roof is emitting a flux quite constant, -87 W/m^2. While the SR appears the heat losses start to rise up until reaching its peak -192 W/m^2, around the same time with the SR peak. After this, its heat losses diminishes until the SR disappears and comes back to its constant behaviour at night.

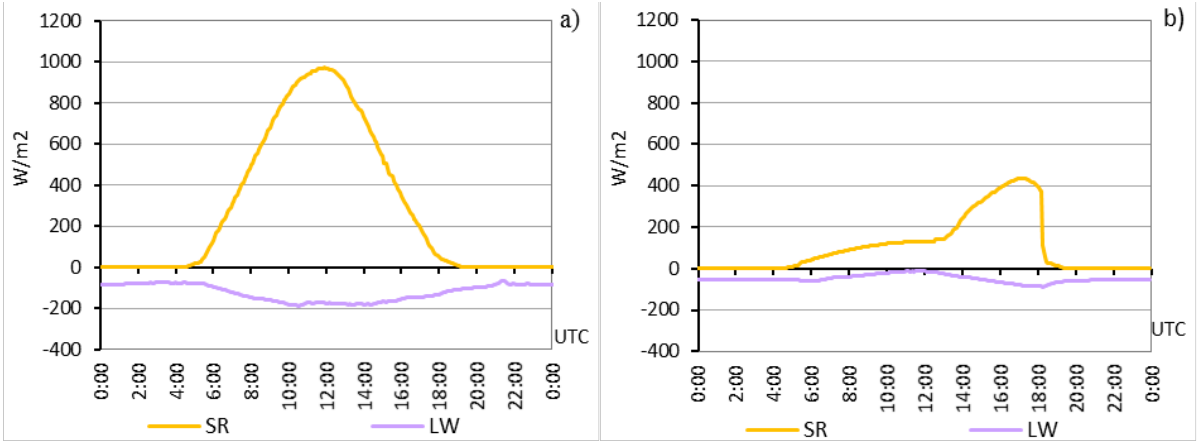

Figure 2. Solar and long wave radiation measured a) on the opaque surface and b) on the glass surface.

There is a relationship among the values of the SR and LW. However, this behaviour gets complicated on the glazed surface due to the roof geometry. The results on the glass surface, Figure 2b, show a SR curve with two different ascending slope. In the morning, the curve keeps a low ascending slope until midday, from 0 to 130 W/m^2. These values reveal the presence of the diffuse-reflect radiation, due to the fact that the glass panels oriented to the North avoid the penetration of the whole direct radiation in this period. After this, SR curve starts to rise with a higher slope until its peak 430 W/m^2, reflecting the incidence of the direct radiation. This behaviour can be observed in Figure 3b, which shows the incidence of the direct radiation only in the afternoon due to the building orientation, 19° to West.

With respect to the LW results, the heat flux is quite constant in the night time periods but with a lower value, -55 W/m^2, than the opaque surface. However in the daytime it displays a totally different behaviour. When solar radiation appears, specifically the diffuse-reflect component, heat losses decrease until -10 W/m^2, around midday. Then, this flux increases until its peak, -87 W/m^2. This responds to direct radiation incidence.

As mentioned, the relationship seen on the opaque part between the SR and LW is not the same in glazed surface results. This behaviour support that the heat losses do not only depend on the amount of the solar radiation received, but also on the heat exchange with its environment. In reference to this, the portion of sky seen by the glass is lower than the one seen by the opaque surface, 55-75% respectively, in terms of Sky View Factor (SVF). Furthermore, the portion of opaque surface seen by the glass has great influence on its heat losses performance due to the high amount of heat flux emitted by the opaque surface, as consequence of the high temperatures it reaches.

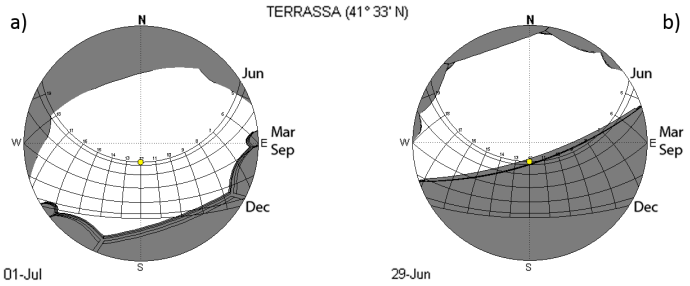

Figure 3. Obstructions of the sun paths in a stereographic projection from the same point of the pyranometer location on the opaque (a) and glass (b) surface. Graphics obtained by Heliodon (Beckers et al, 2003).

In order to analyse the whole heat radiation exchange, the exterior glass and opaque surface temperatures had been measured, Figure 4. At night time periods, these temperatures clearly only depend on heat losses by LW. This is reflected in the temperatures of both surfaces, which keep under the outdoor air temperature due to the high levels of LW emitted to the sky. Moreover, these results shows the influence of the lesser portion of sky seen by the glass compared to opaque part over its surface temperature, which impacts in an average of 2°C higher.

In daytime period, the temperature performance of these two surfaces are conditioned by both radiations: SR and LW. In regards to the opaque part results, these values show a behaviour quite corresponding to their radiation exchange, Figure 2a. In the same way, the results of glass surface temperature show the same pattern seen in the measurements of SR, a curve with two ascending slopes. Nevertheless, these two slopes do not have the large difference seen on radiation results, Figure 2b. With the purpose to analyse this behaviour, it has divided daytime in two periods, morning and afternoon. The average of SR received in the afternoon period is 3 times (255 W/m^2) higher than the one received in the morning (85 W/m^2). Meanwhile the average difference between surface and air temperature, comparing the same periods is 2.5 times, (5°C to 2°C). This behaviour responds to the scarcity of net LW flux emitted in the morning period, which impact in a higher temperature, and transparency of glass to SW.

Regarding the interior surface temperatures results, Figure 4b, the maximum value on both surfaces is around 17:00h. In the case of the opaque surface, it shows a delay of 5 hours and a reduction of 20°C, between the exterior and interior maximum. Meanwhile, in the glass part, the transmission occurs almost immediately, and it displays an increase of its temperature of 7°C. Moreover, the peak on the glass surface temperature is 10°C higher than the one of the opaque part.

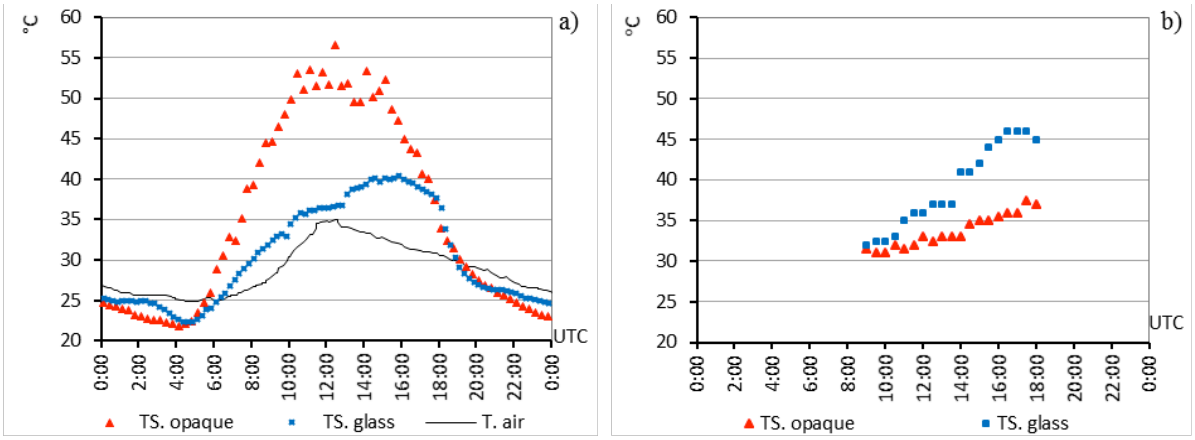

Figure 4. Glass and Opaque Surface temperatures a) exterior and b) interior

Results and discussion: Indoor.

Due to the air velocity measurements obtained (<0.4 m/s), the mean radiant temperature values are considered the same than the globe temperature values (Thorsson et al, 2007). Also, according to these air velocity values the operative temperature is equal to the globe temperature (ASHRAE, 2001).

Figure 5a, shows the indoor results of the air temperature (Tai) and the mean radiant temperature (Tmrt). Neither of these two parameters go under 30°C and their maximums are around 40°C. The indoor temperatures are higher than the outdoor air near the whole day. The average difference between inside and outside is 5°C. Moreover, Tmrt and Tai have the same behaviour and almost the same values in the entire period measured; the highest difference is in their peak time. Figure 5b displays the difference between the Tmrt and Tai (ΔTmrt-Tai). It is observed the range of difference goes from -0.4°C, very constant in night periods, to 1.53°C, in the peak time. Their maximums are around 17:00h, which coincide with the interior temperatures peak of the glass and opaque surfaces, Figure 4b. This reflect the large influence of these surfaces over Tmrt and the influence of this over Tai.

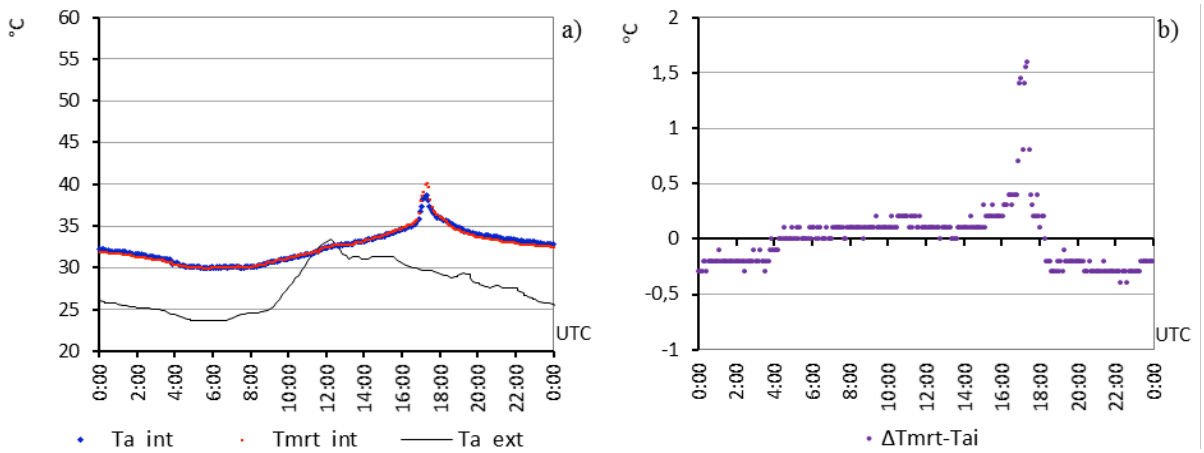

Figure 5. Indoor air temperature and mean radiant indoor temperature (a), and Difference between mean radiant temperature and air temperature (b)

In order to determine the independent impact of the roof surfaces over the interior ambient, it has been calculated the influence of surrounding surfaces over Tmrt. This parameter was calculated based on measured values of the envelope surface temperatures, and their positions respect to the chosen point, shape factor (SF) (Kabre, 2010) obtained from the software Heliodon (Beckers et al, 2003). Equation (1) was used for this purpose:

$$T_{mrt}^4 = \sum_{i=1} T_{si}^4 \cdot F_{pi} \quad (1)$$

Where, T_{mrt} = mean radiant temperature, in K, T_{si} temperature of surface N, in K, F_{pi} angle factor between a point and a surface N. If we refer to the specific case analysed, then the equation can be written as:

$$T_{mrt}^4 = T_{s.op}^4 \cdot F_{p.op} + T_{s.g}^4 \cdot F_{p.g} + T_{s.w}^4 \cdot F_{p.w} + T_{s.f}^4 \cdot F_{p.f} \quad (2)$$

It has simplified the impact of the all surrounding surfaces to one interior point, in 4 surfaces, op = opaque surface, g = glass surface, w = walls, f = floor. Regarding the radiant temperatures, according to the thermal images, Figure 6, the floor and walls have almost the same values than Tai measured, while roof surfaces have higher temperatures. Thus, only roof surfaces are considered in the analysis of the influence over Tmrt. To obtain Ts.g.

and Ts.op. it has been averaged the 9 different points measured over each part. With respect to shape factor parameter, it has been simulated the angle factor between these 4 surfaces and one interior point with the same location of the globe thermometer.

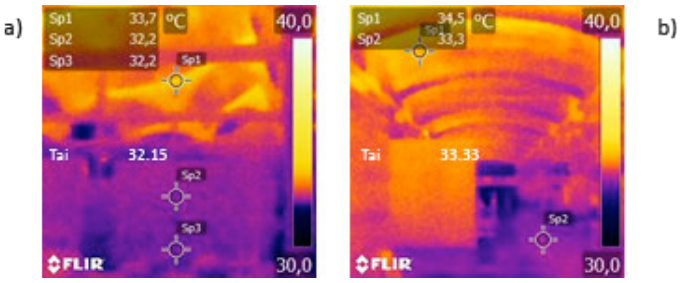

Figure 6 . Interior thermal image 10h00 UTC (a), and 14h00 UTC (b).

Figure 7 shows the difference between the global mean radiant temperature and the mean air temperature (ΔTmrt-Tai), depending on the different values of surrounding temperatures and their shape factors. In the axis X, the range of the surfaces shape factor values, from 0 to 0.5, since 0.5 SF will be the maximum angle factor between the roof and the point analysed. In the axis Y, the values of the difference between surface temperature and air temperature (ΔTs - Tai).

It has been analysed the influence of the Ts.g. and Ts.op. on Tmrt at two different heights: P1: 2.4 m which simulate the same location of globe thermometer, and P2: 4.8 m, a point located in a second floor. The analysis corresponds to temperature peak time, 17:00 h.

According to these results, the glass part has a higher influence over ΔTmrt-Tai than the opaque part on both points analysed. On P1, the influence of the glazed part is 0.84°C and the opaque part is 0.56°C, 60–40% respectively. Meanwhile on P2, the influence, in the same order, are 1.09°C and 0.57°C, 66-34% respectively. It can be observed that when the analysed point gets closer to the roof, the influence of both surfaces over ΔTmrt-Tai becomes higher. However the glass part increases its influence 0.25°C, while the opaque part 0.01°C.

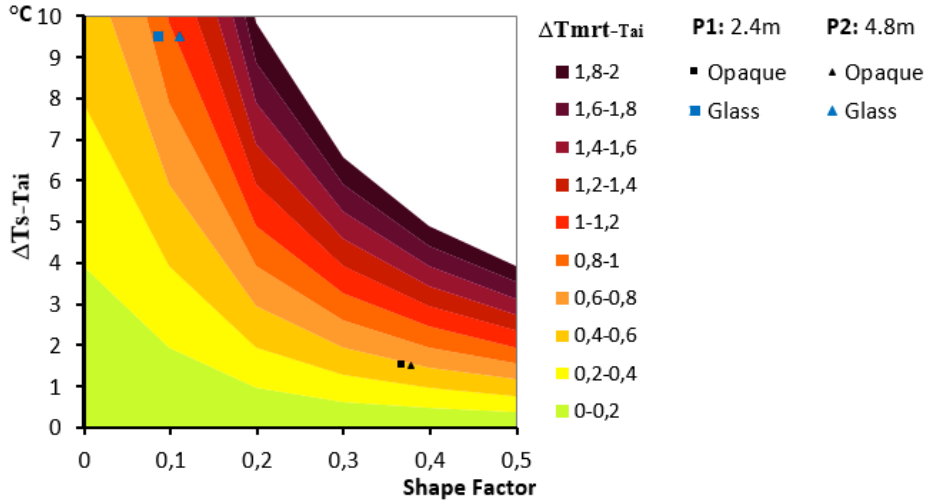

Figure 7. Shape Factor and ΔTs-Ta influence of the surrounding surfaces over Tmrt

Conclusions.

This research approach the analysis of the rehabilitated industrial building interior ambient conditions, focusing in the envelope radiative performance and its impact on the users.

The parameters analysed in this study, Tai and Tmrt, have a strong dependency on the roof thermal behaviour. Considering the whole building volume the highest heat exchange is with the roof surfaces, while the heat flux with the walls and the floor is negligible. In this sense, this analysis supports that the glass surface has the highest repercussion, between the all surfaces of the envelope, over Tmrt. The glass impact represents the 60-66% of the entire long wave radiation flux. This behaviour responds to the high temperatures reached by this surface, 47°C (maximum) although this surface is oriented to the North. These temperatures are determined by the constant action of the diffuse component throughout the whole day, and particularly to the heat radiation emitted by the opaque part, which diminishes the heat losses of this surface.

Acknowledgements.

This work has been supported by the Spanish Ministry of Economy under project code: BIA2016-77675-R. JTQ acknowledges to the scholarship of the SENESCYT ref. AR6C9307 from the government of Ecuador.

References.

Andrei, R. (2012). Industrial building conversion-The Poaching of an already poached reality. *Buletinul Institutului Politehnic Din Iasi*, 58(2), pp. 157-164.

ASHRAE. (2001). ASHRAE Handbook-Fundamentals. Atlanta: ASHRAE

Atmaca, I., Kaynakli, O., Ygit, A. (2007). Effects of radiant temperature on thermal comfort. *Building and Environment*, 42(9), pp. 3210–3220.

Beckers, B., Masset, L. (2003) HeliodonTM_2.6-1 software. Available at: www.heliodon.net.

Beizaee, A., Lomas K., Firth, S. (2013). National survey of summertime temperatures and overheating risk in English homes. *Building and Environment*, 65, pp. 1–17.

Blagojević, M., Tufegdžić, A. (2016). The new technology era requirements and sustainable approach to industrial heritage renewal. *Energy and Buildings*, 115, pp. 148–153.

d'Ambrosio Alfano, F., Dell'Isola, M., Palella, B., Riccio, G., Russi, A. (2013). On the measurement of the mean radiant temperature and its influence on the indoor thermal environment assessment. *Building and Environment,* 63, pp. 79–88.

Fanger, P., Bánhidi, L., Olesen, B., Langkilde, G. (1980). Comfort limits for heated ceilings. *ASHRAE*, 86(2596), pp. 141–156.

Fernández, L., Suárez, L. (2016). Industrial Heritage. Arquitectura Viva, 182, pp. 3.

Givoni, B. (1994). Passive and low energy cooling of buildings. New York: Van Nostrand Reinhold Cop.

Kabre, C. (2010). A new thermal performance index for dwelling roofs in the warm humid tropics. Building and Environment, 45(3), pp. 727–738.

Kalmár, F., Kalmár, T. (2011). Analysis of floor and ceiling heating with intermittent operation. Environmental Engineering and Management Journal, 10(9), pp. 1243–1248.

Kalmár, F., Kalmár, T. (2011). Interrelation between mean radiant temperature and room geometry. Energy & Buildings, 55, pp. 414–421.

Mirzaei, P., Haghighat, F., Nakhaie, A., Yagouti, A., Giguère, M., Keusseyan, R., Coman, A. (2012). Indoor thermal condition in urban heat Island-Development of a predictive tool. *Building and Environment*, 57, p.7–17.

Romeo, E., Morezzi, E., Rudiero, R. (2015) Industrial heritage: Reflections on the use compatibility of cultural sustainability and energy efficiency. *Energy Procedia,* 78, pp.1305-1310

Sutestad, S., Mosler, S. (2016). Industrial Heritage and their Legacies: Memento non mori: Remember you shall not die. *Procedia-Social and Behavioral Sciences*, 225, pp. 321–336. 2016.

Thorsson, S., Lindberg, F. (2007). Different methods for estimating the mean radiant temperature in an outdoor urban setting. *International Journal Climatology,* 27, pp. 1983–1993

Walikewitz, N., Jänicke, B., Langner, M., Meier, F., Endlicher, W. (2015). The difference between the mean radiant temperature and the air temperature within indoor environments : A case study during summer conditions. Building and Environment, 84, pp. 151–161.